Cell

How a Single T Cell Receptor Recognizes Both Self and Foreign MHC

Leremy A. Colf,[1,3] Alexander J. Bankovich,[1,3] Nicole A. Hanick,[1] Natalie A. Bowerman,[2] Lindsay L. Jones,[2] David M. Kranz,[2] and K. Christopher Garcia[1,*]
[1] Howard Hughes Medical Institute, Departments of Molecular and Cellular Physiology, and Structural Biology, Stanford University School of Medicine, Stanford, CA 94305, USA
[2] Department of Biochemistry, University of Illinois at Urbana-Champaign, Urbana, IL 61801, USA
[3] These authors contributed equally to this work.
*Correspondence: kcgarcia@stanford.edu
DOI 10.1016/j.cell.2007.01.048

SUMMARY

αβ T cell receptors (TCRs) can crossreact with both self- and foreign- major histocompatibility complex (MHC) proteins in an enigmatic phenomenon termed alloreactivity. Here we present the 2.35 Å structure of the 2C TCR complexed with its foreign ligand H-2L^d-QL9. Surprisingly, we find that this TCR utilizes a different strategy to engage the foreign pMHC in comparison to the manner in which it recognizes a self ligand H-2K^b-dEV8. 2C engages both shared and polymorphic residues on L^d and K^b, as well as the unrelated QL9 and dEV8 peptide antigens, in unique pair-wise contacts, resulting in greater structural complementarity with the L^d-QL9 complex. In the structure of an engineered, high-affinity 2C TCR variant bound to H-2L^d-QL9, the "wild-type" TCR-MHC binding orientation persists despite modified TCR-CDR3α interactions with peptide. Thus, a single TCR recognizes two globally similar, but distinct ligands by divergent mechanisms, indicating that receptor-ligand crossreactivity can occur in the absence of molecular mimicry.

INTRODUCTION

αβ T cell receptors (TCRs) recognize processed antigenic peptides presented in association with major histocompatibility complex (MHC) proteins (Davis and Bjorkman, 1988). The TCR repertoire is the product of a thymic "education" process during which immature T cells undergo first positive and then negative selection on self (syngeneic, syn) peptide MHC (Starr et al., 2003). Yet, mature T cells exhibit a high frequency of crossreactivity, or alloreactivity (1%–10%) toward foreign (allogeneic, allo) peptide MHC to which they have not been previously exposed during thymic education (Bevan, 1984). The phenomenon of alloreactivity indicates an inherent ability of the TCR to crossreact with a broad range of self- and foreign-pMHC ligands, which could be beneficial for immune surveillance of a universe of potential pathogens (Sherman and Chattopadhyay, 1993). However, it presents a major clinical problem for organ transplantation in that genetically mismatched tissue can be rejected in a graft-host alloresponse. The molecular basis of alloreactivity remains poorly understood, despite the fact that the general structural principles of TCR/pMHC interactions have been greatly advanced by approximately 14 cocrystal structures, (reviewed in Garcia and Adams [2005], Housset and Malissen [2003], Rudolph et al. [2006], and Turner et al. [2006]). More broadly, receptor-ligand crossreactivity has been observed across many systems and has generally been attributed to "molecular mimicry." However, structural evidence for molecular mimicry, in the form of complexes between one receptor and multiple similar, but different ligands, remains elusive for most systems.

The basis of alloreactivity has been extensively debated, and current hypotheses generally converge on either MHC- or peptide-centric mechanisms (Housset and Malissen, 2003; Huseby et al., 2004; Sherman and Chattopadhyay, 1993). In the former, alloreactive TCRs recognize either shared or polymorphic structural determinants on the MHC helices of syn- and allo-MHC with disregard for the peptide (Daniel et al., 1998). This model is in accord with an imprinted "bias" in TCR germline-derived Variable regions for recognition of MHC structural features by virtue of TCR/MHC coevolution (Turner et al., 2006; Zerrahn et al., 1997). There is some structural support for alloreactivity being based on TCR recognition of shared MHC residues. Several crystal structures of allo-pMHC complexes show that the TCR germline-derived CDR1 and CDR2 make identical contacts with the helices in different allo-MHC complexes (Luz et al., 2002; Reiser et al., 2000). A limitation of these studies was either that (1) the allocomplexes could not be compared with the corresponding self complexes or (2) the allo-pMHC molecules were very similar to one another. In the in vivo setting, such as in transplant rejection, TCRs mount

alloresponses to widely different MHC haplotypes and structures. The other mechanism of alloreactivity proposed is that the TCR primarily focuses on the peptide, with only moderate regard for the MHC. Since the current database of TCR/pMHC complex structures contain different TCRs bound to different pMHC, their direct comparisons do not distinguish between effects of the different TCRs and effects of the different peptides. In order to advance our understanding of this issue, it would be informative to elucidate the structure of a single TCR in complex with different self and foreign pMHC.

The 2C TCR represents an ideal system for alloreactivity studies, since the identity of both the self and foreign peptides *and* MHC molecules that positively and negatively select 2C T cells are known (Chen et al., 2003). The self MHC recognized by 2C is H-2K^b, which can positively select 2C T cells when presenting the peptide called dEV8, derived from the enzyme NADH-ubiquinone oxidoreductase (self peptide) (Santori et al., 2002; Tallquist et al., 1998). When K^b is mutated to generate the allo-MHC K^{bm3}, the dEV8/K^{bm3} ligand is converted into a weak agonist for the 2C TCR (Tallquist et al., 1998). Another K^b binding peptide recognized by the 2C TCR, called SIYR, was isolated from a combinatorial peptide library in a screen using peripheral 2C T cells (Udaka et al., 1996). Crystal structures of these three 2C/K^b-peptide complexes showed they were very similar except for minor differences (Figure S1 and Tables S2 and S3) (Degano et al., 2000; Garcia et al., 1998; Luz et al., 2002). These complexes generally exhibit the characteristic TCR/pMHC orientation now seen in other TCR/pMHC complexes, albeit to varying degrees: the CDR1 and 2 of α and β chains primarily lie over the MHC helices, but also contact peptide, while the CDR3 contacts the bound peptide and peptide-proximal regions of the MHC helices (reviewed in Garcia and Adams [2005], Housset and Malissen [2003], and Rudolph et al. [2006]).

2C T cells were originally generated against (Kranz et al., 1984) and are negatively selected (Sha et al., 1988) on the allo-MHC H-2L^d. One of the L^d-associated peptides known to be recognized by 2C is derived from the enzyme α-ketoglutarate dehydrogenase (Udaka et al., 1992). L^d complexes with this self-peptide, p2Ca, and its single amino acid extension QL9, have affinities that are approximately forty-fold higher than H-2K^b-dEV8 (Garcia et al., 1997). The sequence of the QL9 peptide (QLSPFPFDL) is entirely different from dEV8 (EQYKFYSV), and the MHC α1α2 domains of H-2K^b and H-2L^d, which present peptide and are recognized by 2C, differ by 31 residues (Hansen et al., 2000). The H-2L^d helices contain most of the identical residues used by H-2K^b to contact the 2C TCR, but the helices also contain 14 residue polymorphisms. Thus, these structurally divergent foreign- and self-pMHC complexes offer 2C a choice between similar or distinct composite recognition surfaces. Accordingly, structural solutions of this system would be highly informative in advancing our understanding of alloreactivity. Furthermore, alloreactivity is a biologically relevant example of how one protein necessarily crossreacts with many structurally distinct ligands in order to carry out its function. The structural principles, then, of a comparison of distinct self and foreign MHC will expand our understanding of protein-protein crossreactivity in other natural systems.

RESULTS

Previous efforts to obtain cocrystals of 2C/H-2L^d-QL9 were hampered by the instability of H-2L^d and the heterogeneity of the 2C TCR expressed from insect cells. We recently described the in vitro evolution and expression of a stabilized "platform" (α1α2 domains, residues 1–180 of the heavy chain) version of H-2L^d that bypasses the historical problem of poor β_2m association with the α3 domain of the L^d heavy chain (Jones et al., 2006). This platform pMHC molecule exhibits identical affinity and specificity for 2C, as the full-length wild-type H-2L^d-QL9 complex. Through similar in vitro evolution methodologies we have also been able to express a soluble single-chain Fv (VαVβ) version of 2C (Kieke et al., 1999; Shusta et al., 2000). Using these smaller, more stable versions of the TCR and pMHC, we were able to crystallize and solve the structure of the 2C/H-2L^d-QL9 complex at 2.35Å resolution (Table S1 and Figures S2 and S3).

The overall structure of the 2C TCR bound to H-2L^d-QL9 is generally similar to previously determined TCR/pMHC complexes for both class I and class II MHC (Figure 1A). The individual structures of the 2C VαVβ (Fv) module and the platform L^d superimpose closely with their full-length counterparts (root-mean-square deviation [rmsd] of 0.96 Å and 0.81 Å for Cα atoms, respectively) (Figure S2). The orientation places the α chain of the TCR mainly over the α2 helix of the MHC and the center of the peptide, with the β chain of the TCR over the α1 helix and the C terminus of the peptide (Figure 1C). The ~44° 2C/L^d docking orientation, or "footprint," falls within the range seen for complexes of both MHC classes (Garcia and Adams, 2005; Housset and Malissen, 2003; Rudolph et al., 2006; Turner et al., 2006). For the remainder of this paper, we describe this complex only in the context of its relationship to the 2C/H-2K^b-dEV8 complex (Figure 1B), and the attendant implications for alloreactive recognition. Any of the three crystal structures of 2C/H-2K^b-peptide complexes reported suffice for this comparative analysis, as they are similar within the limits of the different resolutions (Figure S1 and Tables S2 and S3). We have chosen H-2K^b-dEV8 as the main comparator because it is a bona fide positive-selecting pMHC complex for the 2C TCR (Santori et al., 2002) and therefore the most direct counterpoint to the 2C/H-2L^d-QL9 complex.

Strikingly, the 2C binding orientations on the syngeneic (H-2K^b-dEV8) and allogeneic (H-2L^d-QL9) pMHC are highly divergent. The footprint of 2C on L^d-QL9 (Figure 1C) is predominantly limited to one helix of the MHC for each TCR chain, while in the 2C/K^b-dEV8 complex, the footprints of each TCR chain span both helices (Figure 1D).

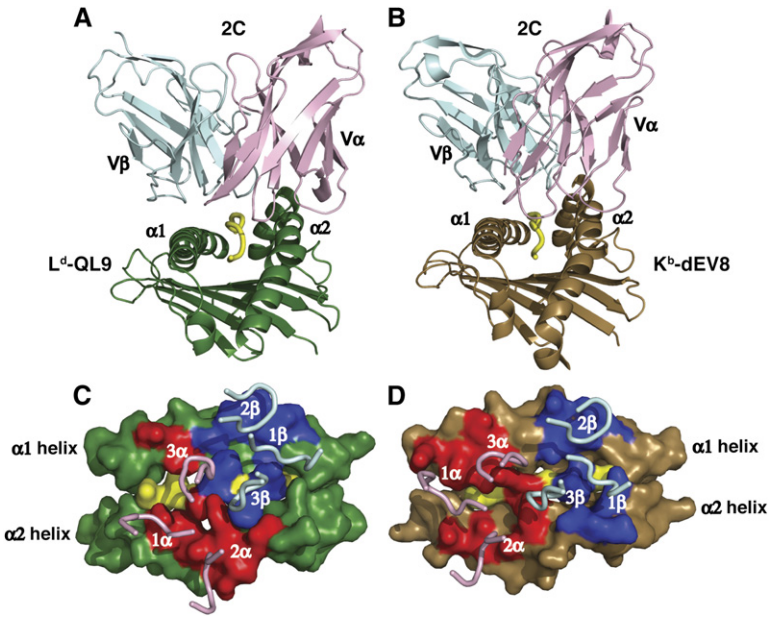

Figure 1. Structure of the 2C TCR in Complex with L^d-QL9

(A) Ribbon diagram of the 2C VαVβ domains complexed with the α1α2 domains of L^d and the QL9 peptide looking down the helical groove of L^d-QL9 (2C Vα is pink, Vβ cyan, L^d green, and peptide yellow).

(B) The 2C VαVβ domains are shown in complex with H-$2K^b$ and the dEV8 peptide. Although the full-length 2C αβ heterodimer and the full-length H-$2K^b$ were solved in that structure (PDBID: 2CKB), we show only the domains corresponding to the 2C/L^d-QL9 complex constructs we used for the current structure. Colors are the same as in (A) except that K^b is brown.

(C and D) The "footprint" view showing the isolated CDR loops of 2C as tubes over the surface rendering of (C) L^d-QL9 and (D) K^b-dEV8. The 2C contact surface on each peptide-MHC is drawn in blue for the Vβ footprint and red for the Vα footprint. Both peptides are yellow. PyMol was used for this and all other structure figures (DeLano, 2002).

Although the 2C/L^d-QL9 complex buries ~275 Å^2 less surface area in the interface than 2C/K^b-dEV8 (1700 Å^2 versus 1975 Å^2, respectively), the 2C/L^d-QL9 interface is mediated by an additional ~111 interatomic contacts (305 for L^d-QL9 and 194 for K^b-dEV8) (Tables S2 and S3). This is due to the more intimately packed interface in 2C/L^d-QL9, which shows a significantly superior shape complementarity (Sc = 0.7) compared to 2C/K^b-dEV8 (Sc = 0.41). 2C contacts with L^d and K^b are both mediated by similar numbers of TCR residues (~23 total: ~11 in Vα and ~12 in Vβ), and 2C buries more surface area with its α chain than its β chain in both complexes (482 Å^2 versus 383 Å^2 in 2C/L^d and 525 Å^2 versus 423 Å^2 in 2C/K^b). In contrast, TCR residues contacting the peptide are dominated by the β chain for QL9 (4α versus 9β), compared to K^b-dEV8 (6α and 6β) and K^{bm3}-dEV8 (7α and 8β). Although the binding geometry differs from a previous model of this complex (Speir et al., 1998), the predominance of β chain contacts in the 2C/L^d interaction is consistent.

When L^d and K^b are structurally superimposed, it is immediately apparent that the 2C footprint on L^d-QL9 is more "perpendicular" than on K^b, relative to the long axis of the MHC groove (Figure 2A). 2C has also translated laterally toward the QL9 C terminus by approximately 3 Å, such that the CDR3s are centered over the P5 position, as compared to the CDR3s centered over the P4 position of dEV8 in K^b. When the same residues on the CDR1 and 2 loops of 2C—in the different complexes—are compared, the Vβ domain is rotated counterclockwise in the allocomplex by approximately 15°, and the Vα domain is rotated approximately 30° (Figure 2A). When the 2C VαVβ domains in each complex are aligned on one another (rmsd of 0.96 for Cα), it is clear that there is a large rotation of the two different pMHC (~20°) with respect to one another in the two complexes (Figure 2B). These rotational and translational shifts result in alternative contacts between 2C/L^d-QL9 relative to the 2C/K^b-dEV8 interface.

For clarity, we schematically depict the relative interactions between 2C CDR loops and the helices of the two different MHC by constructing two-dimensional contact maps (Figures 2C and 2D). Neither CDR1α nor CDR2α of 2C have any interactions with the L^d α1 helix, instead showing extensive interactions with the L^d α2 helix, whereas the CDR1α loop forms numerous contacts with both the α1 and α2 helices of K^b. Correspondingly, CDR1β and CDR2β only contact the α1 helix of L^d, whereas CDR1β and CDR2β form contacts with the α2 and α1 helices in the K^b complex, respectively. When considered in isolation, the 2C shape complementarity with the L^d helices is 0.72 versus 0.48 between 2C and the K^b helices.

The QL9 peptide is bound in an L^d groove, containing a ridge on the peptide binding floor, that is unique to a family of MHC haplotypes (e.g., L^d, L^q, D^q, D^b). This hydrophobic ridge, formed by residues including Trp73 and Tyr99, forces the main chain path of QL9 to arch upwards (Figures 3A, 3C, and S3). Thus, high-affinity peptides for L^d, as well as other MHC in this structural subfamily, bulge out and are therefore typically one extra residue in length (9-mer) in order to traverse the groove (Balendiran et al., 1997). The flatter-lying K^b peptides, such as dEV8, only require eight residues to span the length of the MHC groove (Figures 3B and 3C). The P2-Leu and P9-Leu residues of QL9 appear to form hydrophobic anchors in the core of the groove, while the P4–P7 residues form a projecting bulge that contacts the TCR (Figure 3C). While the main chain indeed forms the bulge, the side chains of P5-Phe, P6-Pro, and P7-Phe fold downward and project outwards toward the L^d helices, resulting in a hydrophobic, propeller-like docking surface on the top of the bulge (Figure 3C), which primarily lies under the 2C Vβ domain. This flat

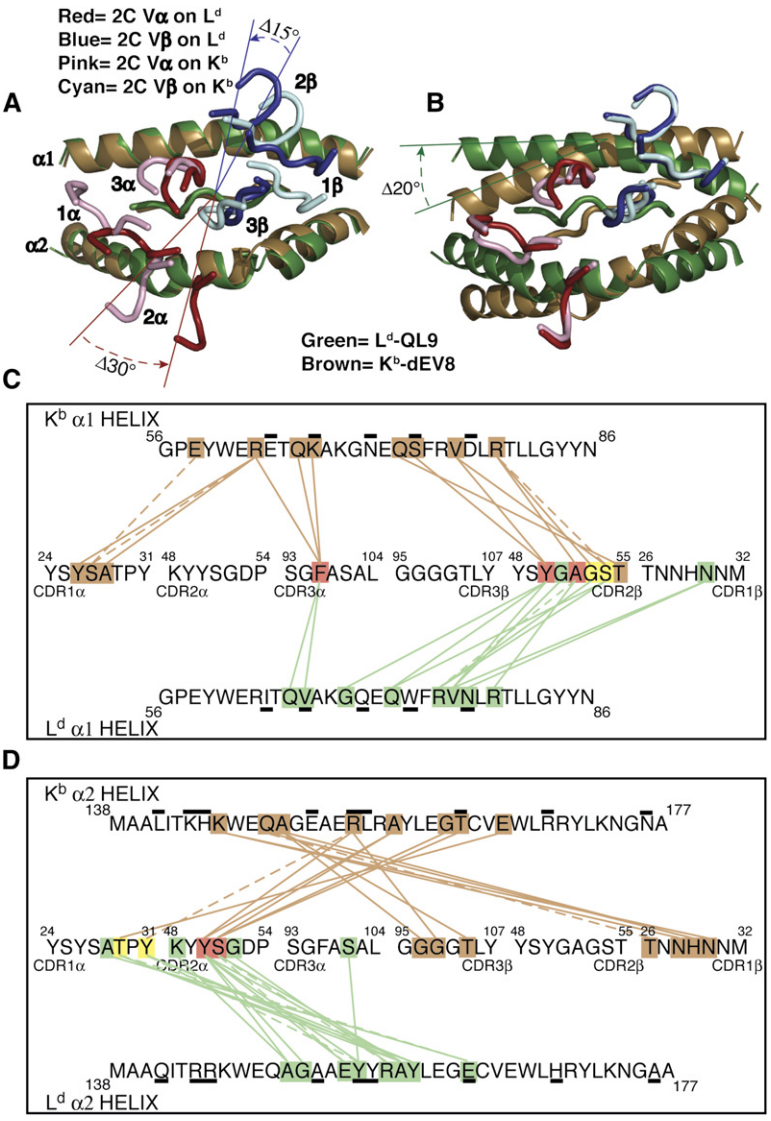

Figure 2. 2C TCR Docking Orientation and Interactions with Its Allogeneic and Syngeneic Ligands

(A) α1α2 domains of L^d-QL9 and K^b-dEV8 in each 2C complex, shown as helical ribbons with peptides, were superimposed (rmsd of 1.03 Å) in order to view the relative positions of the TCR CDR loops. Relative rotational shifts are indicated for Vα and Vβ of 2C (colors are the same as Figure 1).

(B) In the reverse superposition to (A), the 2C VαVβ module was superimposed from each complex (rmsd of 0.96 Å for Cα and 1.29 Å for all atoms) in order to visualize the relative rotations of the MHC helices.

(C and D) Contact maps between the 2C CDR loops (center line) and the L^d (bottom line) and K^b (top line) helices. Panel (C) is for 2C contact with the α1 helix of both MHC, and (D) is for 2C contact with the α2 helix of each MHC. K^b-specific contacts are green, whereas L^d-specific contacts are brown. 2C residues that are present in contacts to both K^b and L^d (regardless of the exact MHC residues) are highlighted in yellow, and 2C residues that contact the identical residue in K^b and L^d are highlighted in red (cross reference with Figure 5C). Solid lines are vdw, and dashed lines are hydrogen bonds. Contacts were based on 4.5 Å cutoff distances and determined in CCP4 using automated criteria.

surface allows the TCR CDR loops to access the pMHC surface without significant structural accommodation of the peptide bulge, even though the peptide main chain does rise higher (~2 Å) out of the groove than the main chain of peptides in K^b.

2C forms a tightly packed interface with the QL9 peptide, using the three CDRs in the β and α chains. 2C uses 13 residues of the TCR (4 in the α chain and 9 in the β chain) to contact 4 residues of the peptide (P4, P5, P7, and P8), resulting in 115 interatomic 2C/QL9 contacts (Figure 3D). The orthogonal orientation rotates the CDR2 loops counterclockwise to roughly twelve and six o'clock, out of range of the most distal QL9 residues in comparison to the more clockwise-rotated 2C/dEV8 complex, where CDR2 of both chains reside at approximately two and eight o'clock and can contact the peptide termini (Figure 2A). The 2C/QL9 contacts are primarily main chain, along with a minority of side-chain specific interactions. The interactions are dominated by van der Waals (vdw) contacts, hydrophobic in nature, with the planar surface created by the P4–P7 bulge, offering little opportunity for H bonding to the CDRs (Figure 4A). For instance, the polyglycine CDR3β (Gly95-Gly96-Gly97-Gly98) covers the P5–P8 span of the peptide (Figures 3A, 3D and S3). Alanine scanning of the QL9 peptide confirms that the P4–P7 positions of QL9 are the most energetically significant residues in the peptide for TCR contact (Figure 5A). The P8-Asp side chain forms three hydrogen bonds, one with Asn-31β and two with the main chains of CDR1β and CDR3β, but replacement of P8-Asp with Ala is only moderately deleterious to binding. This seems to argue against a suggestion that electrostatic interactions between HV4β (Arg69) and P8-Asp of QL9 may account for significant binding energy between the 2C TCR and QL9/L^d (Speir et al., 1998). 2C CDR3α residues Ala101 and Ser102 make van der Waals contacts with QL9

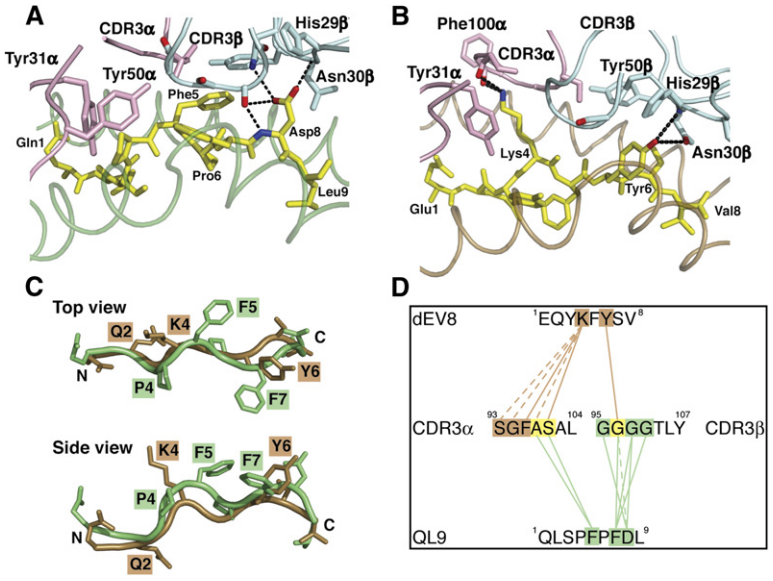

Figure 3. 2C TCR Interactions with the QL9 Peptide

(A) Closeup view of the 2C/QL9 interface, with QL9 shown as yellow sticks. The CDRα and CDRβ loops of 2C are shown (α pink, β cyan) as tubes with sticks and selected residues are labeled. Hydrogen bonds are drawn as dashes.

(B) Same view as (A), except between 2C and the dEV8 peptide.

(C) The isolated QL9 (green) and dEV8 (brown) are shown from the MHC superposition to appreciate the relatively different peptide structures seen by 2C.

(D) Contact map between 2C CDR3s and QL9 and dEV8 peptides, similar to contact map shown in Figures 2C and 2D. 2C CDR3 residues that only contact dEV8 are shown in brown, and QL9 contacts are in green. 2C residues that contact both dEV8 and QL9 are shown in yellow. Solid lines are vdw and dashed lines are hydrogen bonds.

P5-Phe through the inner surface of the loop, but CDR3α also folds away from the peptide to form interactions with a hydrophobic, polymorphic region of the α1 helix of L^d (Gln-Val) (Figure 4A). This observation is consistent with previous studies showing the key influence of QL9 P5-Phe on 2C TCR binding (Schlueter et al., 1996).

This structure clearly illustrates how a single TCR can crossreact with unique peptides. The QL9 and dEV8 peptides are unrelated in sequence, and the 2C intermolecular interactions with the peptides are entirely different in both structure and chemistry (Figures 3A, 3B, and 4A). For example, the interaction between 2C and QL9 is hydrophobic and main-chain directed (Figures 3A and 4A). This contrasts starkly to the polar dEV8 surface, which contacts 2C through extended side-chain H bonds from P1, P2, P4, P6, and P7 positions, some of which are water mediated (Figure 4A). Second, the QL9 peptide is closer to the 2C CDR3 loops due to its higher position in the groove, resulting in a more complementary interface (Sc between QL9 alone and the TCR is 0.7 versus 0.5 for dEV8 alone with 2C). The dEV8 peptide barely contacts 2C through the tips of long extended side chains, leaving large unfilled gaps in the interface. The more intimate 2C/QL9 interface is consistent with the higher affinity of the allogeneic

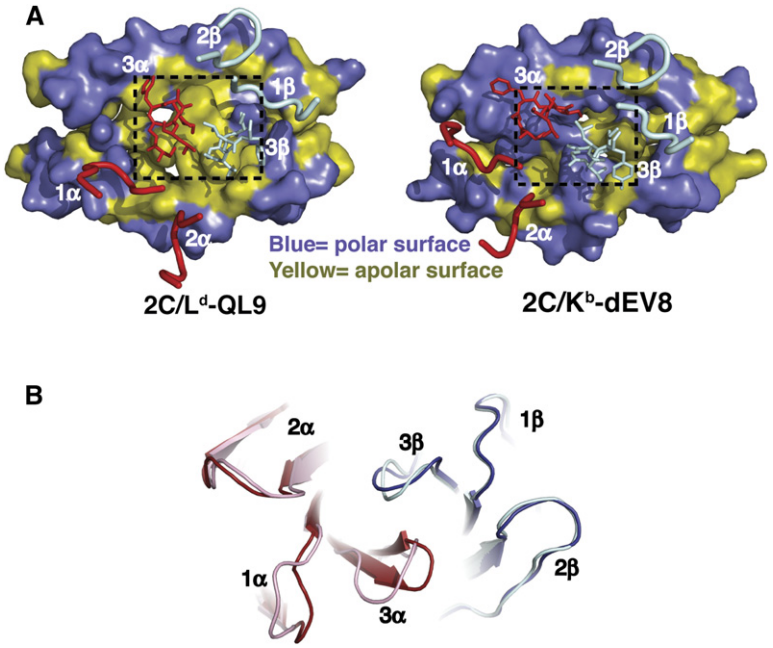

Figure 4. The 2C TCR Contacts Chemically Distinct Peptide-MHC Surfaces in the Absence of Large-Scale Conformational Change in Its CDR Loops

(A) 2C contacts a primarily hydrophobic surface of L^d-QL9 (left) versus a polar surface of K^b-dEV8 (right). The surface of each pMHC bound by 2C has been colored as polar (blue) and apolar (yellow); a dashed box demarcates the location of the CDR3-peptide interactions.

(B) Superimposed 2C TCR from the complex with L^d (TCR α in red, β in blue) and from the complex with K^b (TCR α in pink, β in cyan) showing the relative conformations of the CDR loops.

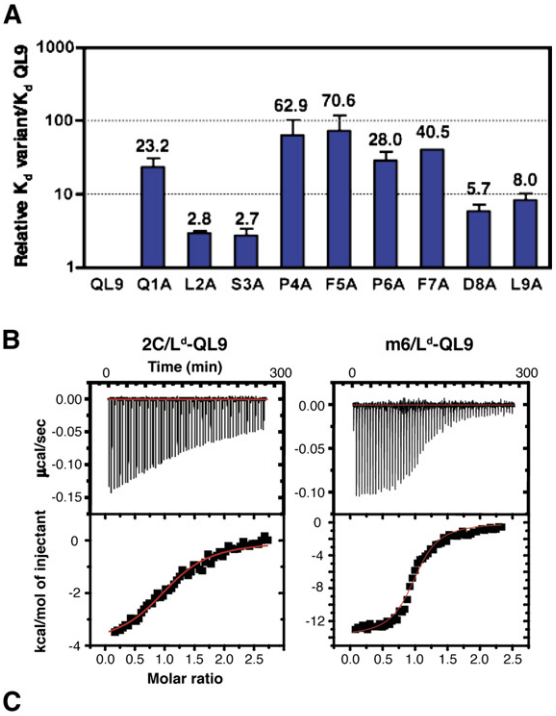

C

2C TCR	Ligand	ΔH kcal/mol	ΔS cal/molK	ΔG kcal/mol	K_d µM
2C sc	L^d-QL9	-4.19	11.58	-7.58	2
m6 sc	L^d-QL9	-13.8	-16.25	-9.04	0.029
2C	K^b-dEV8	-22.7	-54.4	-6.3	83
2C	K^b-SIYR	-8.4	-4.1	-7.2	54
2C	K^b-p2Ca	-29.0	-77.0	-6.1	149

Figure 5. Binding and Thermodynamic Analyses of 2C Binding to Its Syngeneic and Allogeneic Ligands

(A) Alanine scan of the QL9 peptide binding to 2C. 2C TCR tetramers were used in titrations of the indicated QL9 alanine variants bound to L^d, and the binding relative to QL9/L^d was determined. Effects on binding could be either direct (as might be seen for those residues in direct contact with the TCR) or indirect for those residues whose side chains point toward L^d. Error bars represent the standard deviation for two independent experiments (no calculated standard deviation is shown for QL9 F7A, as no binding was detected in one of the experiments).

(B) Isothermal titration calorimetry curves of 2C titrated with L^d-QL9 (left) and m6 titrated with L^d-QL9 (right).

(C) Compilation of 2C binding thermodynamics between the previously measured K^b ligands (Degano et al., 2000; Krogsgaard et al., 2003) and the currently measured allogeneic L^d ligand. The "sc" designation refers to the single-chain Fv constructs used for the 2C/L^d measurements.

interaction versus the syngeneic complex (Garcia et al., 1997; Sykulev et al., 1994). Third, from both the structure and Ala scanning, 2C recognition of QL9 is centered on a C-terminal "hotspot" of the peptide (P4–P7) that bulges upward. By comparison, 2C contacts the flatter dEV8 through side chains spanning almost the entire length of the peptide (P1–P7) (Figure 3B). The more perpendicular orientation of 2C relative to the long axis of the L^d groove results in a shorter stretch of peptide being covered by the TCR (Figure 2A), yet the closer QL9 peptide forms more interatomic contacts (115) than the lower-lying dEV8 peptide (58 contacts).

Previously, the structural plasticity of the TCR CDR3 loops has been noted in comparisons of bound versus free TCR structures (including 2C), revealing both large- and small-scale conformational changes upon binding (Garcia et al., 1998; Reiser et al., 2002). In support of these structural observations, solution measurements reveal entropically disfavored binding between TCR and pMHC (Willcox et al., 1999; Krogsgaard et al., 2003), which has been interpreted as the thermodynamic signature of the entropy penalty incurred during these conformational changes. By extension, it was speculated that CDR3 loop flexibility could be a mechanism enabling a TCR to crossreact with different peptide antigen sequences (Garcia et al., 1998; Reiser et al., 2003). Thus far, however, this concept has not been rigorously tested for recognition of entirely unrelated sequences, as would be encountered in some alloresponses in vivo. Surprisingly, we find that the CDRs of 2C are in remarkably similar conformations in both the QL9 and dEV8 complexes (Figure 4B). The similarities extend to the CDR3s, which show a relatively small local adjustment in the position of the tip of CDR3α (~3 Å), and CDR3β remains essentially the same. The tip of CDR1α has moved approximately 2.5 Å in a rigid body fashion, but the local conformation of the loop is relatively unchanged compared to 2C/K^b (rmsd of 0.92 Å for Cα atoms). Given that the 2C binding site is utilizing similar CDR loop conformations to contact two chemically and structurally unique peptides, we investigated the thermodynamics of 2C interaction with L^d-QL9 for comparison to 2C/K^b-dEV8.

We performed isothermal titration calorimetry (ITC) on 2C with L^d-QL9 for comparison to previously measured values for 2C/H-2K^b-dEV8 (Krogsgaard et al., 2003) (Figures 5B and 5C). Surprisingly, 2C binding to L^d-QL9 is entropically favored, while 2C binding K^b with three different peptides is entropically disfavored and enthalpically driven. The favorable entropy is in accord with the hydrophobic 2C/L^d-QL9 interface, which would likely derive binding energy from expulsion of water from the apolar surfaces (i.e., desolvation), especially the hydrophobic surface of the peptide bulge. The favorable entropy, together with the similarity in CDR loop structure in the two complexes, indicates that additional mechanisms exist to enable TCR crossreactivity other than CDR3 conformational change. Our measurements are consistent with those on shared cytokine receptors and crossreactive natural killer receptors (Boulanger et al., 2003; McFarland and Strong, 2003), which crossreact with different ligands through enthalpy-entropy compensation of rigid binding surfaces and with recent studies with other TCR (Anikeeva et al., 2003; Davis-Harrison et al., 2005; Ely et al., 2006). The study by Ely et al. (2006) showed that a TCR could recognize a pMHC with favorable entropy, even in the presence of some conformational changes (Ely et al., 2006). The broader conclusions of this analysis are that

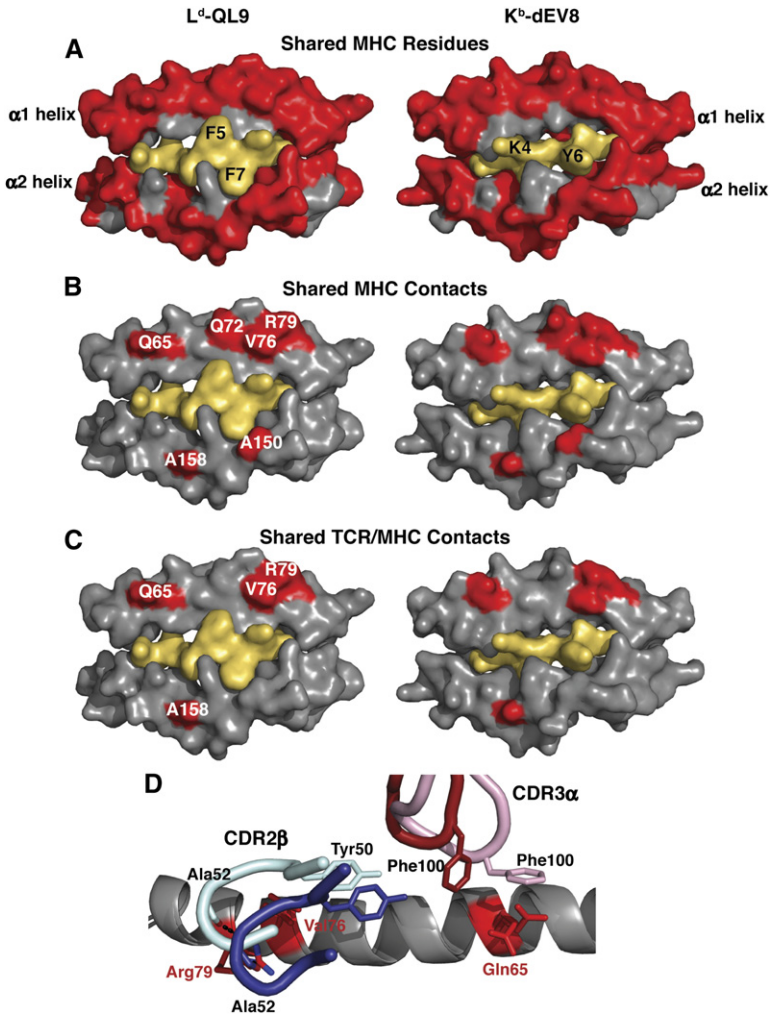

Figure 6. 2C TCR Forms Limited Contacts with Shared Amino Acids on L^d and K^b Recognition Surfaces

(A) Molecular surfaces of L^d-QL9 (left) and K^b-dEV8 (right). Shared residues on the MHC helices are drawn in red.

(B) Only a small subset of the total shared residues shown in (A) are also used as direct contacts with 2C in both complexes.

(C) Of the shared MHC contacts shown in (B), only four also contact the same 2C residue in both complexes.

(D) The common TCR-MHC contacts in (C) are structurally and chemically distinct interactions. Shown are the allogeneic and syngeneic complexes superimposed on the MHC. Three common CDR2β and CDR3α contacts (highlighted in C) are significantly perturbed in each complex such that the bond distances and geometries of the interatomic contacts are different, mainly due to the rotational shift of the CDRs along the MHC helix.

enthalpy-entropy compensation appears to be a potent mechanism to enable receptor crossreactivity in the absence of major conformational changes.

Given the unique binding mode of 2C on L^d-QL9 compared to K^b-dEV8, we wanted to examine the role of shared versus unique MHC residues in dictating the TCR binding orientation. *A priori*, as L^d and K^b share 80% sequence identity in the helices presented to TCR, 2C could either (1) recognize shared residues of L^d and K^b resulting in nearly identical footprints or (2) recognize different residues, resulting in an altered footprint. First we examined the possibility that 2C recognition is determined by the similarities in the two MHC helical surfaces. Although the majority of the 16 K^b residues contacted by 2C are present in L^d (Figure 6A), we found that only six (Gln65, Gln72, Val76, Arg79, Ala150, Ala158) are used as 2C contacts in both complexes, based on a 4.5 Å residue-residue distance criteria to define "contacts" (Figure 6B). From this group and using the same distance criteria, only four residues (Gln65, Val76, Arg79, and Ala158) also contacted the same 2C residues (Figure 6C). We emphasize that, due to the different accuracies of the 2C/K^b-dEV8 complexes, determined at different resolutions, the relative contact analyses vary slightly. For instance, if our contact distance cutoff used to assign interresidue contacts is less than 4 Å (instead of 4.5 Å), there are only two common MHC residues (Val76 and Arg79) contacting the same TCR residues, and at 4.7 Å, there are five common MHC contact residues. Given that "contacts" are assigned purely based on a distance criteria, residues could be within a similar distance but have entirely different contact geometry, chemistry, and stereochemistry. Accordingly, inspection of these apparently conserved TCR-MHC contacts reveals the nature of the interactions, and the atoms utilized are entirely distinct in the L^d versus the three K^b complexes, due to the different TCR/MHC orientation angles (Figure 6D). Thus, the few conserved interactions found in the allogeneic and syngeneic complexes occur via largely unique binding chemistries.

A recent complex of a TCR with a "super-bulged" peptide bound to MHC revealed a "triad" of contacts between the TCR and MHC helices, suggesting this may constitute a minimal MHC structural motif underlying MHC restriction (Tynan et al., 2005). In the case of the 2C complexes with

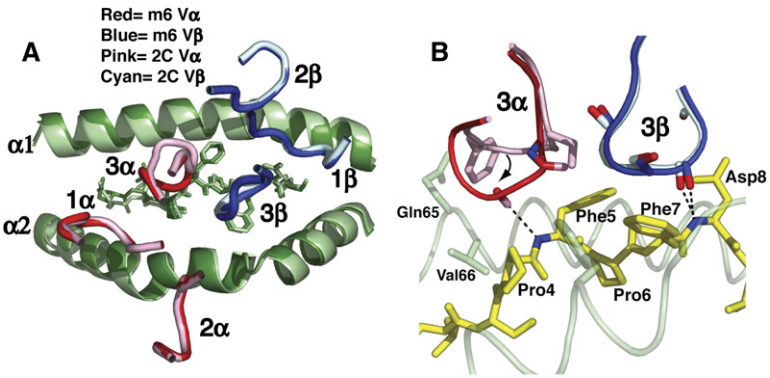

Figure 7. The High-Affinity 2C Variant M6 Has an Identical Footprint to Wild-Type 2C

(A) The high affinity and wild-type complexes were superimposed on L^d-QL9 (rmsd of 0.79 Å for all atoms), showing that the resultant CDR loop positions are identical, except for CDR3α.

(B) M6 CDR3α undergoes a local movement, relative to wild-type 2C, such that its tip folds inward toward the peptide.

K^b and L^d, the distinct interaction chemistries of a roughly similar number of shared TCR-MHC contacts as seen in Tynan et al. (2005) shows that a small subset of MHC residues can be recognized by a single TCR in unique ways when present on different MHC. It would appear, then, that an amino acid "code" underlying MHC bias could be significantly blurred by the possibility of multifarious TCR interactions.

We also analyzed the polymorphic residues presented to the TCR on the surface of the respective syn- and allo-MHC helices. Strikingly, there are only four different residues on the surface of L^d and K^b helices presented to the TCR (66, 145, 155, and 163). The majority of polymorphic residues are in the peptide binding groove, away from the TCR/pMHC interface. Two of the polymorphic residues on the helices, 155 and 163, are contacted in both structures, but 163 is contacted by different CDR loops in the two complexes, while 155 is contacted by the same TCR residues (Tyr31α and Tyr50α) in the two structures (Figures 2C and 2D). Thus, Tyr31α and Tyr50α are among the most energetically important 2C residues in binding the L^d and K^b complexes (Lee et al., 2000; Manning et al., 1998), yet these contributions are associated with contacts to a polymorphic residue. In conclusion, significant sequence conservation between K^b and L^d might have suggested that the most parsimonious recognition strategy by 2C for L^d would have been a K^b-like footprint. However the interatomic contacts are almost entirely different based on analysis of pair-wise amino acid contacts.

Tail Wagging the Dog, or Dog Wagging the Tail?

The structural results and analysis so far could implicate a "peptide-centric" model of alloreactivity, whereby recognition of the QL9 peptide has steered the TCR into an alternative footprint on the MHC. In this model, the specific TCR-peptide interactions would "edit" the overall TCR docking footprint, as was suggested from analysis of human autoimmune and antiviral TCR/pMHC complexes (Borg et al., 2005; Hahn et al., 2005). However, this interpretation of our results is contradicted by energetic mapping (Ala scanning) of 2C residues in the 2C/L^d-peptide versus 2C/K^b-peptide interactions, which indicate that most energetically significant binding determinants are derived from CDR1 and CDR2, which mainly contact the helices in both the allo- and syngeneic complexes (Lee et al., 2000; Manning et al., 1998). Conceptually, the peptide-centric model can be thought of as a "tail wagging the dog" in that the TCR-peptide (tail) contacts seem to determine the TCR CDR1 and CDR2 footprint on the MHC helices (the dog). This model stands in contrast to the MHC-centric models (dog wagging the tail) whereby shared structural determinants on MHC, recognized by TCR CDR1 and CDR2, determine the ultimate docking mode.

We tested whether the tail is wagging the dog or the dog is wagging the tail. We have previously evolved, using yeast display, a high-affinity variant of 2C through mutation of CDR3α (Holler et al., 2000), which contacts both QL9 and L^d in the structure. The evolution experiment is "unbiased" in that recombinant TCR and pMHC were used in vitro, in the absence of T cell coreceptors (e.g., CD8/CD4) that could influence the binding orientation, as has been proposed (Buslepp et al., 2003). Thus, the TCR has, in principle, freedom to assume any docking footprint on L^d-QL9 as a result of the remodeled CDR3-peptide interactions. By producing a new CDR3α sequence that will form unique interactions with the peptide MHC, we can ask whether the CDR1 and CDR2 contacts with MHC have been edited in deference to perturbed CDR3-peptide interactions. In other words, is the tail wagging the dog?

The in vitro evolution of 2C into a high-affinity variant, termed m6, which retains specificity for L^d-QL9, has been described previously (Holler et al., 2000). M6 has a CDR3α sequence of SHQGRYL (compared to wild-type SGFASAL) and recognizes L^d-QL9 with high affinity as measured both by surface plasmon resonance (Jones et al., 2006) and ITC (Figures 5B and 5C). Interestingly, m6 has incurred an entropic penalty for binding H-2L^d-QL9, so the binding chemistry has changed in both amino acid sequence and thermodynamics. We crystallized m6 in complex with L^d-QL9 and determined the structure to 2.5 Å resolution (Table S1). The overall binding orientation of the TCR on L^d-QL9 is identical to 2C/L^d-QL9 (the entire complexes superimpose with an rmsd of 0.79 Å for all atoms) (Figure 7A), with the five wild-type CDR loops forming identical contacts with L^d and QL9. The only significant structural difference is the position of the CDR3α loop,

whose tip is now displaced 4.5 Å inward toward the peptide compared to the wild-type 2C complex (Figure 7B). This inward displacement results in a decrease in interactions with the L^d α1 helix, instead focusing its contacts on QL9 residues P4 and F5. The mode of interaction is hydrophobic, whereby aliphatic groups of CDR3α residues Gln100, Gly101, and Arg102 form van der Waals contacts with the planar surface previously described for the bulged peptide residues. The location and conformation of CDR3β is identical in the two structures. Thus, despite focusing completely new, higher-affinity binding energetics on the peptide by directed evolution of CDR3α, the wild-type binding orientation persists. Our principal conclusion is that although the TCR footprint on L^d-QL9 is unique relative to K^b-dEV8, it is not simply a result of editing by QL9 peptide/CDR3 interactions. 2C recognition of L^d-QL9 occurs through a discrete binding solution, which persists in the face of perturbed peptide-CDR3 contacts. In short, for the case of 2C alloreactivity, the dog appears to be wagging the tail.

DISCUSSION

We show that one receptor, 2C, has at least two possible binding orientations—"suboptimal" and "optimal"—on its self- and foreign-peptide-MHC ligands, respectively, which present both similar and distinct surfaces for the TCR to recognize. In addition, binding to self and foreign ligands was achieved through different chemistries and thermodynamic mechanisms. The starkly contrasting mechanisms by which 2C recognizes two distinct, naturally occurring ligands is broadly informative about multispecific protein interactions. Even when different ligands present similar constellations of receptor binding residues (i.e., possess significant homology), the receptor need not utilize a similar recognition strategy to crossreact. For the case of an adaptive immune receptor such as the TCR, which we presumed would "home" to conserved, shared structural determinants on the MHC ligands with which it has coevolved, the majority of the recognition strategy focused on *differences* between the ligands. Thus, other mechanisms than molecular mimicry can explain cross-reactivity in the natural setting. Further, the aberrant self reactivity characteristic of autoimmune diseases need not arise through molecular mimicry even in cases of microbial antigens that strongly resemble self proteins (Wucherpfennig and Strominger, 1995). The generality of the 2C mechanism of allorecognition, to other TCR systems, awaits further structure function studies of TCRs whose cognate and allo-pMHC ligands are known (Archbold et al., 2006).

From an immunological standpoint, we conclude that 2C alloreactivity can be considered a "synthesis" of the peptide- and MHC-centric hypotheses. We suggest that the germline-encoded contacts between TCR and MHC, which have been selected through coevolution (Huseby et al., 2004; Jerne, 1971; Turner et al., 2006; Zerrahn et al., 1997), play the dominant role in dictating the overall binding geometry. However, different allo- and self-peptides presented by the MHC may influence the TCR to select one *preferred* orientation, out of a defined *set* of possible germline-encoded footprints, that is compatible with making contacts with a specific peptide to produce a physiologically meaningful affinity (K_D ~1–50 μM). Thus, we predict that each peptide does not recruit a TCR to form "de novo" footprints with the MHC helices that are not among the germline-encoded set. In support of this, a previous study showed that different TCRs that both contained Vβ8.2 formed identical docking contacts on the $I\text{-}A^u$ and $I\text{-}A^k$ MHC helices, despite different peptides and CDR3 sequences (Maynard et al., 2005).

An important question is whether the optimal TCR/MHC docking orientation we see in the 2C/L^d complex would be seen on self MHC (K^b) if K^b were presenting a foreign peptide. The SIYR peptide is a foreign peptide that reacts with 2C in the context of K^b (Udaka et al., 1996), and that fits the criteria of a peripherally selected cognate ligand. The structure of 2C bound to H-$2K^b$-SIYR has been reported (Degano et al., 2000) and is nearly identical to those of other 2C/K^b complexes (Figure S1). Thus, 2C does not recognize the strong agonist peptide-MHC K^b-SIYR, with a significantly different strategy than other 2C/K^b-peptide complexes. The strong agonist activity of SIYR/K^b is accomplished despite a relatively low affinity (K_D ~30 μM) for the 2C TCR, especially compared to QL9/L^d. However, we have shown previously that the relative agonist activities of the various peptides (dEV8, SIYR, p2Ca, and QL9) are dictated largely by the stabilities of the peptide-MHC complexes (Holler and Kranz, 2003; Krogsgaard et al., 2003).

Does this docking orientation extend to other TCRs that are involved in L^d recognition? A previous L^d mutational analysis supports this possibility, in that different T cells appear to contact a conserved set of helix residues on L^d, implying that this orientation may be generalized (Hornell et al., 1999). Furthermore, the Vβ8 region appears to be used preferentially with a number of L^d-restricted responses and the p2Ca/QL9-L^d ligands in particular (Connolly, 1994; Rodewald et al., 1989; Tjoa and Kranz, 1994).

The present study shows that alloreactions are not only due to molecular mimicry, but they are also a consequence of less predictable interactions with alloantigens that have more significant structural diversity than the syngeneic MHC. While the 2C/L^d-QL9 interaction is CD8 independent, the role of coreceptor in influencing TCR/MHC orientation remains an important consideration (Buslepp et al., 2003). Recent findings that 2C and other class I-restricted TCRs can recognize class II products may yield even more alternative docking orientations (Ge et al., 2006), presumably dependent on yet other chemistries, for their productive interactions.

EXPERIMENTAL PROCEDURES

Protein Expression and Purification

The 2C TCR, as well as the high-affinity 2C mutant, m6, was expressed as a soluble, single-chain construct by *E. coli* periplasmic expression

as described (Jones et al., 2006). Briefly, proteins were expressed from the pET22b vector as Vα-$(Gly_4Ser)_4$ linker-Vβ single chains with a C-terminal His_6 purification tag. Mutations in Vβ8.2 were included to increase solubility (G17E, H47Y, I75T, and L81S). Protein was expressed in BL21 (DE3) Codon Plus *E. coli* (Stratagene) and purified by Nickel NTA affinity chromatography and gel filtration as described (Jones et al., 2006).

A version of the H-2L^d class I MHC containing only the α1α2 domains was expressed by refolding from *E. coli* inclusion bodies as described (Jones et al., 2006). Inclusion bodies were expressed in BL21 (DE3) Codon Plus *E. coli* (Stratagene) and refolded in the presence of excess QL9, and the complex was purified by gel filtration. The platform L^d used for crystallization with 2C contained three additional hydrophobic-to-polar mutations (F9Y, V12T, and I23T) in a surface patch on the underside of the β sheet, which is normally in contact with β_2M and α3 domains. These polar surface substitutions increased its solubility in aqueous buffers but are far removed from the TCR binding interface and had no effect on its 2C binding properties.

Crystallization, Data Collection, and Processing

Purified TCR and pMHC were combined in equimolar amounts and concentrated in a YM10 Centriprep (Amicon) to approximately 50 mg/ml for each of the complexes (2C/L^d-QL9 and m6/L^d-QL9). Crystals were obtained in 0.9 M sodium dihydrogen phosphate and 0.1 M dipotassium hydrogen phosphate (2C/L^d-QL9) or 0.2 M ammonium phosphate, 20% polyethyleneglycol (PEG) 3350, and 0.1 M Tris at pH 8.5 (m6/L^d-QL9) using the sitting drop vapor diffusion method. Crystals were cryoprotected using 25% glycerol (2C/L^d-QL9) or 30% PEG 3350 (m6/L^d-QL9) before cooling to 100 K. Data were collected on beamline 11.1 at the Stanford Synchrotron Light Source (SSRL, Stanford, CA). Crystals of 2C/L^d-QL9 diffracted to 2.35 Å, cell dimensions a = 163.2 Å, b = 163.2 Å, c= 95.0 Å, in space group $P6_522$. Crystals of m6/L^d-QL9 diffracted to 2.5 Å, cell dimensions a = 113.5 Å, b = 113.5 Å, c = 177.5 Å, space group $P4_22_12$. The data were indexed, integrated, and scaled with HKL2000 (Otwinowski and Minor, 1997).

Structure Solution and Refinement

Complex structures were determined by molecular replacement with the program Phaser (Read, 2001). Protein Data Bank (PDB) files 1LDP (for L^d) and 2CKB (for the TCR) were used as search models after trimming coordinates to correspond to the smaller molecules used to crystallize the 2C/L^d-QL9 complex, searching sequentially with the TCR α chain, TCR β chain, and MHC. One round of rigid body refinement was performed, followed by rounds of model building using COOT (Emsley and Cowtan, 2004), simulated annealing, and positional and individual B factor refinements using the CNS software package (Brunger et al., 1998), resulting in R and free R values of 22.0% and 22.6%, respectively.

Individual components of the completed 2C/L^d-QL9 model were used as search models for the m6/L^d-QL9 molecular replacement. After refinement by similar methodologies, the resultant R and free R values were 22.4% and 24.6%, respectively. A summary of refinement statistics is given in Table S1.

Isothermal Titration Calorimetry

Protein expression and purification for isothermal titration calorimetry were similar to that for crystallography, except that TCR samples were treated overnight with carboxypeptidase A and B at 4°C prior to size-exclusion chromatography. All proteins were purified in the same buffer (10 mM HEPES, 150 mM NaCl, pH 7.2) to minimize heat of dilution effects. Thermodynamic parameters were determined using a VP-ITC calorimeter (MicroCal, Northhampton, MA) at 20°C. Protein samples were degassed prior to titrations. Data were processed using MicroCal Origin 5.0 software. Titrations were performed with a range of concentrations. Conditions giving the strongest signal with the lowest background were L^d-QL9 (185 μM) injected into 2C (45 μM) and L^d-QL9 (52 μM) injected into m6 (5 μM). Experiments at other concentrations yielded similar thermodynamic parameters (data not shown).

2C scTCR Binding to QL9 Variants

Relative binding affinities of the 2C scTCR for L^d bound to QL9 variants were determined using 2C scTCR tetramers and peptide-loaded L^d on target cells, as has recently been described (Huseby et al., 2006). Single-site alanine variants of QL9 (100 μM) were incubated with cell line T2-L^d for 3 hr at 37°C. Peptide-loaded cells were incubated with various concentrations of tetrameric 2C scTCR (T7) for 40 min at 4°C. Streptavidin-PE (BD Pharmingen) labeled TCR was detected using a Coulter Epics XL flow cytometer. K_d values of QL9 variants relative to QL9 wt were determined by nonlinear regression of the equilibrium binding curves, using a value (50 mean fluorescent units) in the linear range of the curves. Values were corrected for total L^d levels using the anti-L^d Ab 30-5-7, and background was subtracted for 2C scTCR binding to the null ligand MCMV/L^d. Error bars represent the standard deviation (SD) for two independent experiments (no calculated SD is shown for QL9 F7A, as no detectable binding was detected in one of the experiments).

Supplemental Data

Supplemental Data include three figures and three tables and can be found with this article online at http://www.cell.com/cgi/content/full/129/1/135/DC1/.

ACKNOWLEDGMENTS

We thank Sean Juo for assistance with structure determination; Phil Holler and Susan Brophy for generation of the m6 TCR and the m31 L^d mutants, respectively; and Herman Eisen for his advice and previous studies on the 2C system. We also gratefully acknowledge the staff and resources of the SSRL. L.C. is supported by an National Science Foundation predoctoral fellowship. This work was supported by NIH grants AI 48540 (K.C.G.) and GM55767 (D.M.K.). K.C.G. is also supported by the Keck Foundation and Howard Hughes Medical Institute.

Received: November 23, 2006
Revised: January 1, 2007
Accepted: January 19, 2007
Published: April 5, 2007

REFERENCES

Anikeeva, N., Lebedeva, T., Krogsgaard, M., Tetin, S.Y., Martinez-Hackert, E., Kalams, S.A., Davis, M.M., and Sykulev, Y. (2003). Distinct molecular mechanisms account for the specificity of two different T-cell receptors. Biochemistry *42*, 4709–4716.

Archbold, J.K., Macdonald, W.A., Miles, J.J., Brennan, R.M., Kjer-Nielsen, L., McCluskey, J., Burrows, S.R., and Rossjohn, J. (2006). Alloreactivity between disparate cognate and allogeneic pMHC-I complexes is resultant of highly focused, peptide-dependent structural mimicry. J. Biol. Chem. *281*, 34324–34332.

Balendiran, G.K., Solheim, J.C., Young, A.C., Hansen, T.H., Nathenson, S.G., and Sacchettini, J.C. (1997). The three-dimensional structure of an H-2Ld-peptide complex explains the unique interaction of Ld with beta-2 microglobulin and peptide. Proc. Natl. Acad. Sci. U.S.A. *94*, 6880–6885.

Bevan, M.J. (1984). High determinant density may explain the phenomenon of alloreactivity. Immunol. Today *5*, 128.

Borg, N.A., Ely, L.K., Beddoe, T., Macdonald, W.A., Reid, H.H., Clements, C.S., Purcell, A.W., Kjer-Nielsen, L., Miles, J.J., Burrows, S.R., et al. (2005). The CDR3 regions of an immunodominant T cell receptor dictate the 'energetic landscape' of peptide-MHC recognition. Nat. Immunol. *6*, 171–180.

Boulanger, M.J., Bankovich, A.J., Kortemme, T., Baker, D., and Garcia, K.C. (2003). Convergent mechanisms for recognition of divergent cytokines by the shared signaling receptor gp130. Mol. Cell *12*, 577–589.

Brunger, A.T., Adams, P.D., Clore, G.M., DeLano, W.L., Gros, P., Grosse-Kunstleve, R.W., Jiang, J.S., Kuszewski, J., Nilges, M., Pannu, N.S., et al. (1998). Crystallography & NMR system: A new software suite for macromolecular structure determination. Acta Crystallogr. D Biol. Crystallogr. *54*, 905–921.

Buslepp, J., Wang, H., Biddison, W.E., Appella, E., and Collins, E.J. (2003). A correlation between TCR Valpha docking on MHC and CD8 dependence: implications for T cell selection. Immunity *19*, 595–606.

Chen, J., Eisen, H.N., and Kranz, D.M. (2003). A model T-cell receptor system for studying memory T-cell development. Microbes Infect. *5*, 233–240.

Connolly, J.M. (1994). The peptide p2Ca is immunodominant in allorecognition of L^d by β chain variable region $V\beta8^+$ but not $V\beta8^-$ strains. Proc. Natl. Acad. Sci. USA *91*, 11482–11486.

Daniel, C., Horvath, S., and Allen, P.M. (1998). A basis for alloreactivity: MHC helical residues broaden peptide recognition by the TCR. Immunity *8*, 543–552.

Davis, M.M., and Bjorkman, P.J. (1988). T-cell antigen receptor genes and T-cell recognition. Nature *334*, 395–402.

Davis-Harrison, R.L., Armstrong, K.M., and Baker, B.M. (2005). Two different T cell receptors use different thermodynamic strategies to recognize the same peptide/MHC ligand. J. Mol. Biol. *346*, 533–550.

Degano, M., Garcia, K.C., Apostolopoulos, V., Rudolph, M.G., Teyton, L., and Wilson, I.A. (2000). A functional hot spot for antigen recognition in a superagonist TCR/MHC complex. Immunity *12*, 251–261.

DeLano, W.L. (2002). The PyMOL Molecular Graphics System (San Carlos, CA, USA: DeLano Scientific).

Ely, L.K., Beddoe, T., Clements, C.S., Matthews, J.M., Purcell, A.W., Kjer-Nielsen, L., McCluskey, J., and Rossjohn, J. (2006). Disparate thermodynamics governing T cell receptor-MHC-I interactions implicate extrinsic factors in guiding MHC restriction. Proc. Natl. Acad. Sci. USA *103*, 6641–6646.

Emsley, P., and Cowtan, K. (2004). Coot: model-building tools for molecular graphics. Acta Crystallogr. D Biol. Crystallogr. *60*, 2126–2132.

Garcia, K.C., and Adams, E.J. (2005). How the T cell receptor sees antigen–a structural view. Cell *122*, 333–336.

Garcia, K.C., Degano, M., Pease, L.R., Huang, M., Peterson, P., Teyton, L., and Wilson, I.A. (1998). Structural basis of plasticity in T cell receptor recognition of a self peptide-MHC antigen. Science *279*, 1166–1172.

Garcia, K.C., Tallquist, M.D., Pease, L.R., Brunmark, A., Scott, C.A., Degano, M., Stura, E.A., Peterson, P.A., Wilson, I.A., and Teyton, L. (1997). Alphabeta T cell receptor interactions with syngeneic and allogeneic ligands: affinity measurements and crystallization. Proc. Natl. Acad. Sci. USA *94*, 13838–13843.

Ge, Q., Holler, P.D., Mahajan, V.S., Nuygen, T., Eisen, H.N., and Chen, J. (2006). Development of CD4+ T cells expressing a nominally MHC class I-restricted T cell receptor by two different mechanisms. Proc. Natl. Acad. Sci. USA *103*, 1822–1827.

Hahn, M., Nicholson, M.J., Pyrdol, J., and Wucherpfennig, K.W. (2005). Unconventional topology of self peptide-major histocompatibility complex binding by a human autoimmune T cell receptor. Nat. Immunol. *6*, 490–496.

Hansen, T., Balendiran, G., Solheim, J., Ostrov, D., and Nathenson, S. (2000). Structural features of MHC class I molecules that might facilitate alternative pathways of presentation. Immunol. Today *21*, 83–88.

Holler, P.D., and Kranz, D.M. (2003). Quantitative analysis of the contribution of TCR/pepMHC affinity and CD8 to T cell activation. Immunity *18*, 255–264.

Holler, P.D., Holman, P.O., Shusta, E.V., O'Herrin, S., Wittrup, K.D., and Kranz, D.M. (2000). In vitro evolution of a T cell receptor with high affinity for peptide/MHC. Proc. Natl. Acad. Sci. USA *97*, 5387–5392.

Hornell, T.M., Solheim, J.C., Myers, N.B., Gillanders, W.E., Balendiran, G.K., Hansen, T.H., and Connolly, J.M. (1999). Alloreactive and syngeneic CTL are comparably dependent on interaction with MHC class I alpha-helical residues. J. Immunol. *163*, 3217–3225.

Housset, D., and Malissen, B. (2003). What do TCR-pMHC crystal structures teach us about MHC restriction and alloreactivity? Trends Immunol. *24*, 429–437.

Huseby, E., Kappler, J., and Marrack, P. (2004). TCR-MHC/peptide interactions: kissing-cousins or a shotgun wedding? Eur. J. Immunol. *34*, 1243–1250.

Huseby, E.S., Crawford, F., White, J., Marrack, P., and Kappler, J.W. (2006). Interface-disrupting amino acids establish specificity between T cell receptors and complexes of major histocompatibility complex and peptide. Nat. Immunol. *7*, 1191–1199.

Jerne, N.K. (1971). The somatic generation of immune recognition. Eur. J. Immunol. *1*, 1–9.

Jones, L.L., Brophy, S.E., Bankovich, A.J., Colf, L.A., Hanick, N.A., Garcia, K.C., and Kranz, D.M. (2006). Engineering and characterization of a stabilized alpha1/alpha2 module of the class I major histocompatibility complex product Ld. J. Biol. Chem. *281*, 25734–25744.

Kieke, M.C., Shusta, E.V., Boder, E.T., Teyton, L., Wittrup, K.D., and Kranz, D.M. (1999). Selection of functional T cell receptor mutants from a yeast surface- display library. Proc. Natl. Acad. Sci. USA *96*, 5651–5656.

Kranz, D.M., Sherman, D.H., Sitkovsky, M.V., Pasternack, M.S., and Eisen, H.N. (1984). Immunoprecipitation of cell surface structure of cloned cytotoxic T lymphocytes by clone-specific antisera. Proc. Natl. Acad. Sci. USA *81*, 573–577.

Krogsgaard, M., Prado, N., Adams, E.J., He, X.L., Chow, D.C., Wilson, D.B., Garcia, K.C., and Davis, M.M. (2003). Evidence that structural rearrangements and/or flexibility during TCR binding can contribute to T cell activation. Mol. Cell *12*, 1367–1378.

Lee, P.U., Churchill, H.R., Daniels, M., Jameson, S.C., and Kranz, D.M. (2000). Role of 2C T cell receptor residues in the binding of self- and allo- major histocompatibility complexes. J. Exp. Med. *191*, 1355–1364.

Luz, J.G., Huang, M., Garcia, K.C., Rudolph, M.G., Apostolopoulos, V., Teyton, L., and Wilson, I.A. (2002). Structural comparison of allogeneic and syngeneic T cell receptor-peptide-major histocompatibility complex complexes: a buried alloreactive mutation subtly alters peptide presentation substantially increasing V(beta) Interactions. J. Exp. Med. *195*, 1175–1186.

Manning, T.C., Schlueter, C.J., Brodnicki, T.C., Parke, E.A., Speir, J.A., Garcia, K.C., Teyton, L., Wilson, I.A., and Kranz, D.M. (1998). Alanine scanning mutagenesis of an alphabeta T cell receptor: mapping the energy of antigen recognition. Immunity *8*, 413–425.

Maynard, J., Petersson, K., Wilson, D.H., Adams, E.J., Blondelle, S.E., Boulanger, M.J., Wilson, D.B., and Garcia, K.C. (2005). Structure of an autoimmune T cell receptor complexed with class II peptide-MHC: insights into MHC bias and antigen specificity. Immunity *22*, 81–92.

McFarland, B.J., and Strong, R.K. (2003). Thermodynamic analysis of degenerate recognition by the NKG2D immunoreceptor: not induced fit but rigid adaptation. Immunity *19*, 803–812.

Otwinowski, Z., and Minor, W. (1997). Processing of X-ray diffraction data collected in oscillation mode. Methods Enzymol *276*, 307–326.

Read, R.J. (2001). Pushing the boundaries of molecular replacement with maximum likelihood. Acta Crystallogr. D Biol. Crystallogr. *57*, 1373–1382.

Reiser, J.B., Darnault, C., Guimezanes, A., Gregoire, C., Mosser, T., Schmitt-Verhulst, A.M., Fontecilla-Camps, J.C., Malissen, B., Housset, D., and Mazza, G. (2000). Crystal structure of a T cell receptor bound to an allogeneic MHC molecule. Nat. Immunol. *1*, 291–297.

Reiser, J.B., Gregoire, C., Darnault, C., Mosser, T., Guimezanes, A., Schmitt-Verhulst, A.M., Fontecilla-Camps, J.C., Mazza, G., Malissen, B., and Housset, D. (2002). A T cell receptor CDR3beta loop undergoes conformational changes of unprecedented magnitude upon binding to a peptide/MHC class I complex. Immunity *16*, 345–354.

Reiser, J.B., Darnault, C., Gregoire, C., Mosser, T., Mazza, G., Kearney, A., van der Merwe, P.A., Fontecilla-Camps, J.C., Housset, D., and Malissen, B. (2003). CDR3 loop flexibility contributes to the degeneracy of TCR recognition. Nat. Immunol. *4*, 241–247.

Rodewald, H.R., Koszinowski, U.H., Eichmann, K., and Melchers, I. (1989). Predominant utilization of V beta 8+ T cell receptor genes in the H-2Ld- restricted cytotoxic T cell response against the immediate-early protein pp89 of the murine cytomegalovirus. J. Immunol. *143*, 4238–4243.

Rudolph, M.G., Stanfield, R.L., and Wilson, I.A. (2006). How TCRs bind MHCs, peptides, and coreceptors. Annu. Rev. Immunol. *24*, 419–466.

Santori, F.R., Kieper, W.C., Brown, S.M., Lu, Y., Neubert, T.A., Johnson, K.L., Naylor, S., Vukmanovic, S., Hogquist, K.A., and Jameson, S.C. (2002). Rare, structurally homologous self-peptides promote thymocyte positive selection. Immunity *17*, 131–142.

Schlueter, C.J., Manning, T.C., Schodin, B.A., and Kranz, D.M. (1996). A residue in the center of peptide QL9 affects binding to both L^d and the T cell receptor. J. Immunol. *157*, 4478–4485.

Sha, W.C., Nelson, C.A., Newberry, R.D., Kranz, D.M., Russell, J.H., and Loh, D.Y. (1988). Positive and negative selection of an antigen receptor on T cells in transgenic mice. Nature *336*, 73–76.

Sherman, L.A., and Chattopadhyay, S. (1993). The molecular basis of allorecognition. Annu. Rev. Immunol. *11*, 385–402.

Shusta, E.V., Holler, P.D., Kieke, M.C., Kranz, D.M., and Wittrup, K.D. (2000). Directed evolution of a stable scaffold for T-cell receptor engineering. Nat. Biotechnol. *18*, 754–759.

Speir, J.A., Garcia, K.C., Brunmark, A., Degano, M., Peterson, P.A., Teyton, L., and Wilson, I.A. (1998). Structural basis of 2C TCR allorecognition of H-2Ld peptide complexes. Immunity *8*, 553–562.

Starr, T.K., Jameson, S.C., and Hogquist, K.A. (2003). Positive and negative selection of T cells. Annu. Rev. Immunol. *21*, 139–176.

Sykulev, Y., Brunmark, A., Tsomides, T.J., Kageyama, S., Jackson, M., Peterson, P.A., and Eisen, H.N. (1994). High-affinity reactions between antigen-specific T-cell receptors and peptides associated with allogeneic and syngeneic major histocompatibility complex class I proteins. Proc. Natl. Acad. Sci. USA *91*, 11487–11491.

Tallquist, M.D., Weaver, A.J., and Pease, L.R. (1998). Degenerate recognition of alloantigenic peptides on a positive- selecting class I molecule. J. Immunol. *160*, 802–809.

Tjoa, B.A., and Kranz, D.M. (1994). Sequence restrictions in T cell receptor β-chains that have specificity for a self-peptide/L^d complex. Mol. Immunol. *31*, 705–711.

Turner, S.J., Doherty, P.C., McCluskey, J., and Rossjohn, J. (2006). Structural determinants of T-cell receptor bias in immunity. Nat. Rev. Immunol. *6*, 883–894.

Tynan, F.E., Burrows, S.R., Buckle, A.M., Clements, C.S., Borg, N.A., Miles, J.J., Beddoe, T., Whisstock, J.C., Wilce, M.C., Silins, S.L., et al. (2005). T cell receptor recognition of a 'super-bulged' major histocompatibility complex class I-bound peptide. Nat. Immunol. *6*, 1114–1122.

Udaka, K., Tsomides, T.J., and Eisen, H.N. (1992). A naturally occurring peptide recognized by alloreactive CD8+ cytotoxic T lymphocytes in association with a class I MHC protein. Cell *69*, 989–998.

Udaka, K., Wiesmuller, K., Kienle, S., Jung, G., and Walden, P. (1996). Self-MHC-restricted peptides recognized by an alloreactive T-lymphocyte clone. J. Immunol. *157*, 670–678.

Willcox, B.E., Gao, G.F., Wyer, J.R., Ladbury, J.E., Bell, J.I., Jakobsen, B.K., and Anton van der Merwe, P.A. (1999). TCR binding to peptide-MHC stabilizes a flexible recognition interface. Immunity *10*, 357–365.

Wucherpfennig, K.W., and Strominger, J.L. (1995). Molecular mimicry in T cell-mediated autoimmunity: viral peptides activate human T cell clones specific for myelin basic protein. Cell *80*, 695–705.

Zerrahn, J., Held, W., and Raulet, D.H. (1997). The MHC reactivity of the T cell repertoire prior to positive and negative selection. Cell *88*, 627–636.

Accession Numbers

The 2C/L^d-QL9 and m6/L^d-QL9 coordinates have been deposited in the PDB with accession numbers 2OI9 and 2E7L, respectively.